

Preparation and Characterization of Nanostructured $\text{CaCu}_{2.90}\text{Zn}_{0.10}\text{Ti}_4\text{O}_{12}$ Ceramic

Regular Paper

Laxman Singh¹, U. S. Rai¹ and K. D. Mandal^{2,*}

¹ Department of Chemistry, Faculty of Science, Banaras Hindu University, India

² Department of Applied Chemistry, Institute of Technology, Banaras Hindu University, India

* Corresponding author: kdmandal.apc@itbhu.ac.in

Received 11 May, 2011; Accepted 16 December, 2011

Abstract Nanostructure $\text{CaCu}_{2.90}\text{Zn}_{0.10}\text{Ti}_4\text{O}_{12}$ (CCZTO) electronic ceramic was synthesized by semi-wet route. The objective of this route is to enable the calcination and sintering processes to go for completion in shorter time and at lower temperature. The samples were characterized by XRD, TEM, SEM and EDX analyses. The crystallite size of the CCZTO ceramic, obtained by XRD using Debye Scherrer formula, range from 38-74nm which is in good agreement with the particle size observed by TEM analysis. It was observed clearly that the grain size significantly increased with an increase in sintering duration. Dielectric measurements were carried out by LCR meter in the temperature range, 300- 500K, at few selected frequencies. It was also observed that the dielectric constant and dielectric loss of CCZTO are temperature independent in higher frequency whereas temperature dependent in low frequency region. The ceramics exhibit high dielectric constant of 1.35×10^4 at 1 kHz.

Keywords Ceramics, nanoparticles, dielectric properties

1. Introduction

Nanosized materials with high dielectric constant are in the focus of interest, not only for purely academic reasons

but also because new high ϵ_r materials are urgently sought for the further development of modern electronics. The high dielectric constant material is desirable to miniaturize capacitor required for integrated circuit. BaTiO_3 and SrTiO_3 based ferroelectric materials exhibit high dielectric constant but these materials show strong temperature dependence of their dielectric constant which is not desirable from the device points of view [1-2]. On the other hand, $\text{CaCu}_3\text{Ti}_4\text{O}_{12}$ (CCTO) ceramic has high dielectric constant ($\epsilon_r \sim 10^4 - 10^5$) independent of frequency ($10^2 - 10^6$ Hz) and temperature (100-600K) which is desired for microelectronic applications [3-4]. Unfortunately, the CCTO ceramic with giant dielectric constant exhibits higher dielectric loss that limits its practical applications. It has been previously reported that the dielectric properties of CCTO are largely influenced by factors such as doping schemes [5-7] as well as stoichiometric variations [8-9]. Recently much work based on partial substitution at Cu or Ti ions site in CCTO ceramic has been carried out in order to improve the dielectric properties and to understand the origin of giant dielectric response in $\text{CaCu}_3\text{Ti}_4\text{O}_{12}$ ceramic [10-12]. Partial isovalent ionic substitutions of Cu by Zn or Mg in $\text{CaCu}_3\text{Ti}_4\text{O}_{12}$ ceramic have enhanced the dielectric response due to modification of its structure [13-15]. In these cases,

compared to the slight change of $\text{Cu}^+/ \text{Cu}^{2+}$ ratio which also increases $\text{Ti}^{3+}/ \text{Ti}^{4+}$ ratio, may be the primary factor for the enhanced dielectric response in CCTO ceramic. The dielectric constant (ϵ_r) and loss tangent ($\tan\delta$) of CCTO are strongly dependent upon the processing conditions such as sintering temperature [16], sintering time [17], cooling rate and partial pressure of sintering atmosphere. The traditional solid-state reaction method is usually used to prepare crystalline CCTO with starting materials, CaCO_3 , CuO and TiO_2 , in stoichiometric ratio at high temperature. The mixtures are calcined for long duration with several intermediate grindings. This procedure requires tedious work, relatively long reaction time and high temperature condition. In addition, some other secondary phases also appear during synthesis because of limited atomic diffusion through micrometer sized grains. On the other hand, the wet chemical methods provide atomic level mixing of individual components and result in the formation of nanocrystalline materials at much lower temperature compared with solid state reactions. There are many chemical methods, such as, sol-gel, co-precipitation, precursor solution technique and hydrothermal process [18–20] which have already been reported for the synthesis of CCTO ceramics. But in these chemical methods Ti is used as $\text{Ti}(\text{OR})_4$ which is very costly.

In the present communication we report a new successful route to synthesize nanocrystalline CCZTO by semi-wet route at low sintering temperature and short duration. In this method, the mixing process is performed in solution state as nitrate solutions along with solid TiO_2 which is very cheap. This is one of the most advantages over the other methods. We also report the dielectric properties of this ceramic.

2. Experimental

Analytical grade chemicals, $\text{Ca}(\text{NO}_3)_2 \cdot 4\text{H}_2\text{O}$, $\text{Cu}(\text{NO}_3)_2 \cdot 3\text{H}_2\text{O}$, $(\text{CH}_3\text{COO})_2\text{Zn} \cdot 2\text{H}_2\text{O}$, titanium dioxide and citric acid, obtained from Merk, having purity of 99.95 % or better were used as starting materials. Standard solutions of metal nitrates were prepared using distilled water. Solutions of the metal nitrates in stoichiometric amount of these metallic ions were mixed in a beaker. Calculated amounts of TiO_2 and citric acid equivalent to metal ions were added to the solution. The solution was heated on a hot plate using a magnetic stirrer at 70–90 °C to evaporate water and then dried at 100–120°C in hot air oven for 12h to yield a blue gel. The gel was calcined in air at 800°C for 6h in a muffle furnace. The resultant mixture was ground into fine powder using a pestle and mortar. Cylindrical pellets were made using hydraulic press. The pellets, sintered at 950 °C for 6 h, 8h and 12h in air, were abbreviated as CCZTO-6h, CCZTO-8h and CCZTO-12h, respectively. The densities of samples were measured by Archimedes method. The

crystalline phases of the sintered samples were identified using an X-ray Diffractometer (Rich-Siefert, ID-3000) employing $\text{Cu-K}\alpha$ radiation. The microstructures of the fractured surfaces were examined using a Scanning Electron Microscope (SEM, Model JEOL JSM5410). The Energy Dispersive X-ray Analyzer (EDX, Model KeveX, Sigma KS3) was used for the elemental analysis of the sintered samples. Transmission Electron Microscopic (TEM Technai 12 G2, FEI) studies of the sintered samples were carried out by placing the test sample on carbon-coated copper grid, operated at an accelerated voltage of 120 kV. The dielectric data of Zn doped CCTO ceramics were collected using the LCR meter (PSM 1735, Newton 4th Ltd, U.K) with variation in temperature at few selected frequencies.

3. Results and discussion

The relative densities of $\text{CaCu}_{2.90}\text{Zn}_{0.10}\text{Ti}_4\text{O}_{12}$ (CCZTO) ceramics sintered at 6h, 8h and 12h were found to be 91.16, 93.34 and 94.44%, respectively. It clearly shows that density increases with sintering time. XRD patterns of $\text{CaCu}_{2.90}\text{Zn}_{0.10}\text{Ti}_4\text{O}_{12}$ sintered at 950 °C with different sintering time (6h, 8h and 12h) are shown in Fig.1. X-Ray data were indexed on the basis of a cubic unit cell similar to undoped CCTO (JCPDS 75-2188), which confirm the formation of single phase. The lattice parameters and unit cell volume, determined using least square refinement method, are given in Table 1.

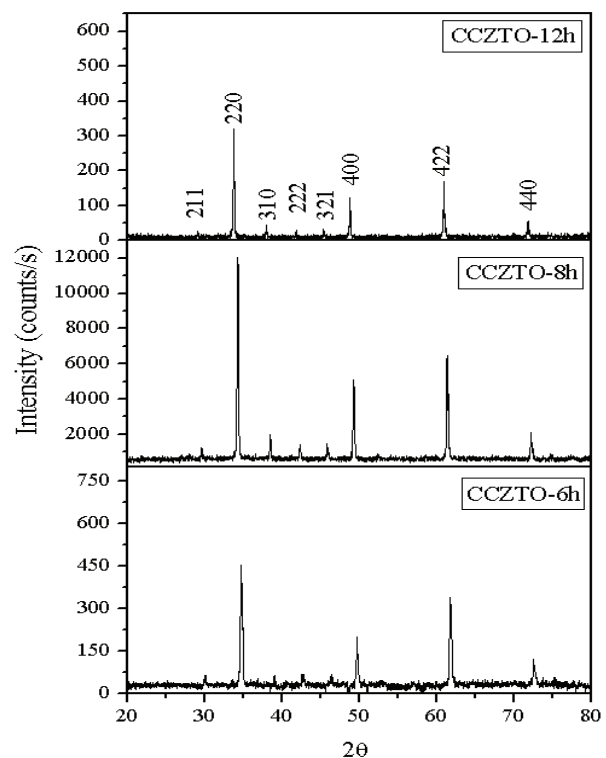


Figure 1. X-ray diffraction patterns of $\text{CaCu}_{2.90}\text{Zn}_{0.10}\text{Ti}_4\text{O}_{12}$ Ceramics sintered at 950 °C for 6h, 8h and 12h

Sintering time	Lattice Parameter (Å)	Lattice Volume (Å ³)	Crystallite size from XRD (nm)	Particle size from TEM (nm)
6h	7.276±0.256	385	38± 13	54± 11
8h	7.321±0.008	392	69± 16	73± 23
12h	7.378±0.015	401	74± 18	84± 15

Table 1. Lattice parameter, unit cell volume and particle size obtained from XRD and TEM for CaCu_{2.90}Zn_{0.10}Ti₄O₁₂

Fig. 2 shows the variation of lattice parameter with sintering time. It is observed from the figure that the lattice parameter increases with the increase in the sintering time. The change in unit cell parameter with time of annealing is due to increase in density. During the heat treatment each crystallite get enough dwelling time to get properly crystallized [21].

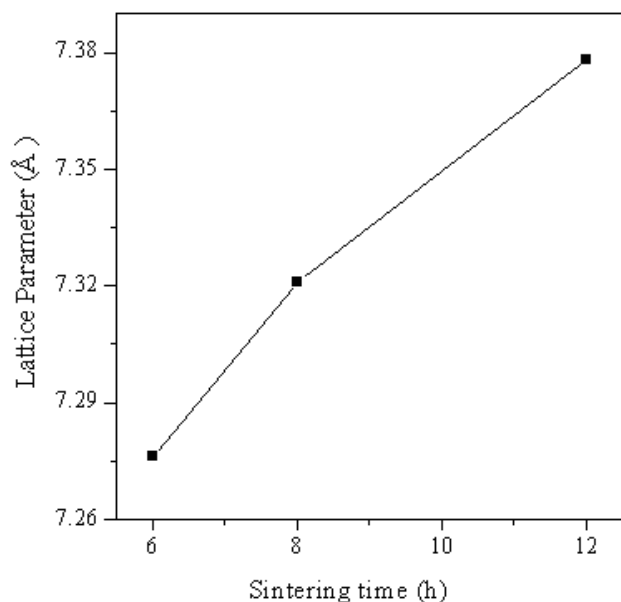


Figure 2. Variation of lattice parameter with sintering time

There is no evidence of the presence of secondary phase. XRD patterns show the presence of split peaks for the reflections at 400, 422 and 440. This may be due to presence of Cu-Kα₂ along with Cu-Kα₁ in the X-ray radiations used for the diffraction. This is supported by the fact that in all these reflections the intensity of peaks due to Cu-Kα₂ is close to 50 % of intensity of peak due to Cu Kα₁ as expected. From the line broadening of the main peaks, the crystallite size of the ceramic was estimated using the Debye Scherrer formula [22] :

$$D = k \lambda / \beta \cos \theta \quad (1)$$

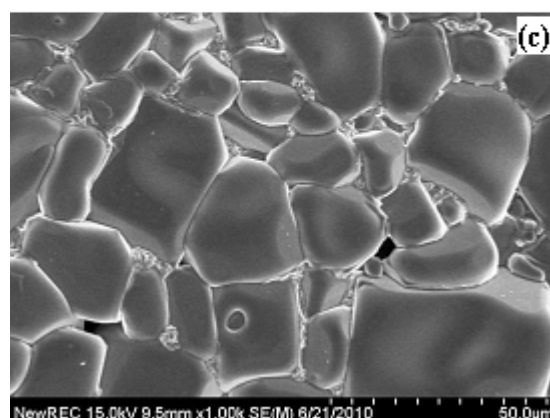
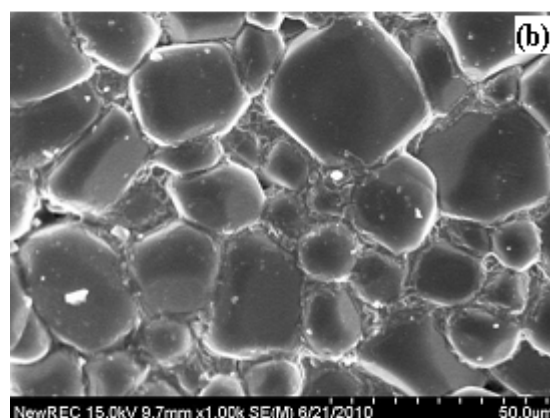
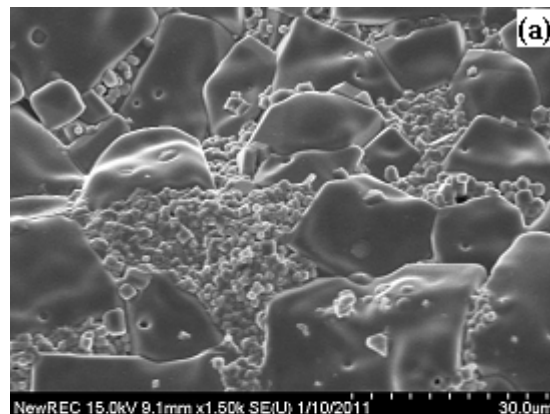


Figure 3. SEM images of CCZTO ceramics sintered at 950 °C for (a) 6h , (b) 8h and (c) 12h

where λ is the wavelength of the X-ray, k is a constant taken as 0.89, θ is the diffraction angle and β is the full width at half maxima (FWHM). The crystallite size derived from the XRD data and TEM analysis are given in the Table 1.

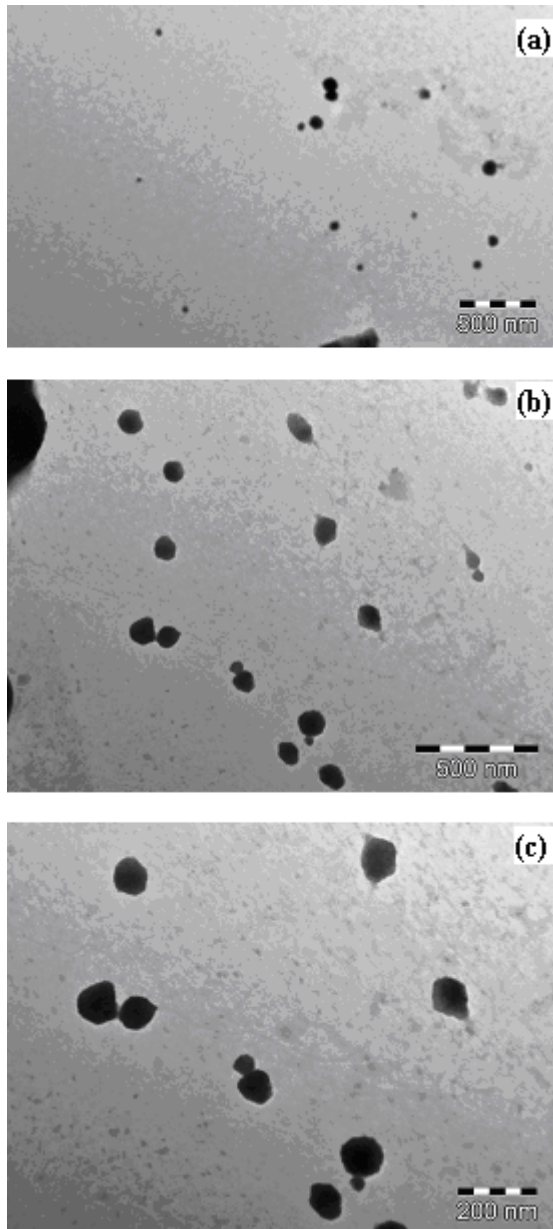


Figure 4. TEM images of CCZTO ceramics sintered at 950 °C for (a) 6h , (b) 8h and (c) 12h

It is clearly observed that the crystallite size increased with increasing sintering duration, which is confirmed by the TEM analysis. The increased crystallite size with increasing sintering time is mainly due to over grown grains resulting from the destruction of the grain boundaries at higher sintering time. These data clearly show that the sintering time is responsible for increasing crystallite size with increasing sintering time of $\text{CaCu}_{2.90}\text{Zn}_{0.10}\text{Ti}_4\text{O}_{12}$ ceramic.

Fig. 3 shows SEM images of surface microstructures for the ceramics sintered at different sintering times. As can be seen from Fig. 3(a)-(c), the microstructures of $\text{CaCu}_{2.9}\text{Zn}_{0.1}\text{Ti}_4\text{O}_{12}$ change significantly with sintering time. In specimen sintered at 950 °C for 6h a porous with

small grain size 8-10 μm is observed. The grain size range varies from 10-15 μm and 15-25 μm of the ceramics sintered at 8h and 12h, respectively. It can be seen that the grain size increased with increase of sintering time and the correspondingly grain boundary was reduced. Increasing the sintering time significantly promotes the grain growth and microstructural densification. The microstructures show grain growth in the specimen sintered for 8h and 12h along with some liquid phase. Additionally, a small amount of CuO phase was found in grain boundary region. This phase was so small that XRD could not detect. It also seems that with increasing sintering time from 6h, 8h and 12h solid CuO phase start melting as shown in Fig. 3(b) and totally melted in at grain boundary as shown in Fig. 3(c). Copper oxide present at grain-boundary transforms into the liquid phase during sintering which leads to abnormal grain growth [23-24].

TEM images (Fig. 4) of the CCZTO sintered powders clearly show that all of the samples consist of nanocrystalline CCZTO particles whose size increases with increasing sintering time. A representative manually constructed histogram of particle size distribution of $\text{CaCu}_{2.90}\text{Zn}_{0.10}\text{Ti}_4\text{O}_{12}$ (CCZTO-8h) is shown in Fig.5. The particle size of the ceramics sintered at 950 °C for 6h, 8h and 12h were found to be 54 ± 11 , 73 ± 23 and 84 ± 15 nm, respectively. The crystallite size obtained using Debye Scherrer formula is smaller than the particle size obtained by TEM. This is due to fact that the Debye Scherrer formula does not take into account the effect of lattice strain and instrumental factors on peak broadening.

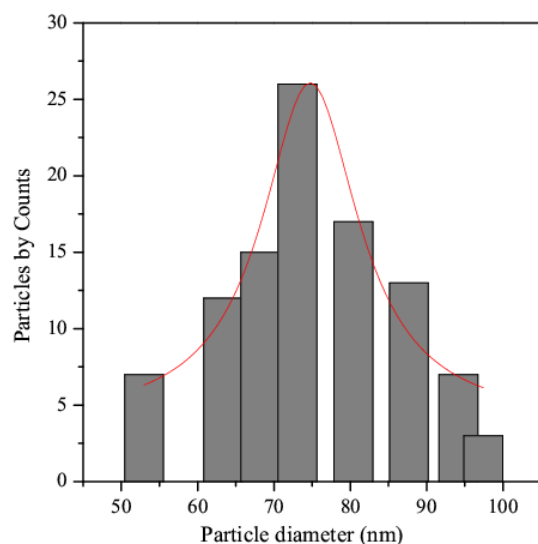


Figure 5. Histogram of Particle size distribution curve of $\text{CaCu}_{2.90}\text{Zn}_{0.10}\text{Ti}_4\text{O}_{12}$ nanoparticles of CCZTO-8h

EDX spectra of CCZTO ceramic (Fig.6) sintered at 950 °C for 6h, 8h and 12h show the presence of Ca, Cu, Zn, Ti and an extra peak of Pt at 2.15 keV. Pt coating was

performed by ion beam sputtering for increasing the conductivity which was necessary to avoid charging or charged up of samples. The atomic percentage of Ca, Cu, Zn and Ti in the CCZTO ceramics obtained from EDX data are given in Table 2. The Cu/Ca ratio for CCZTO-6h, CCZTO-8h and CCZTO-12h are 2.75, 2.73 and 2.73, respectively. The percentage error are found to be 5.45, 6.22 and 6.22%, respectively.

Sintering duration	Atomic % of elements				
	Ca	Cu	Zn	Ti	O
6h	4.76	13.11	0.38	17.04	64.71
8h	6.69	18.33	0.67	25.90	48.41
12h	6.72	18.37	0.70	24.29	49.92

Table 2. Atomic percentage of elements for $\text{CaCu}_{2.90}\text{Zn}_{0.10}\text{Ti}_4\text{O}_{12}$ (CCZTO) sintered at 950 °C for 6h, 8h and 12h

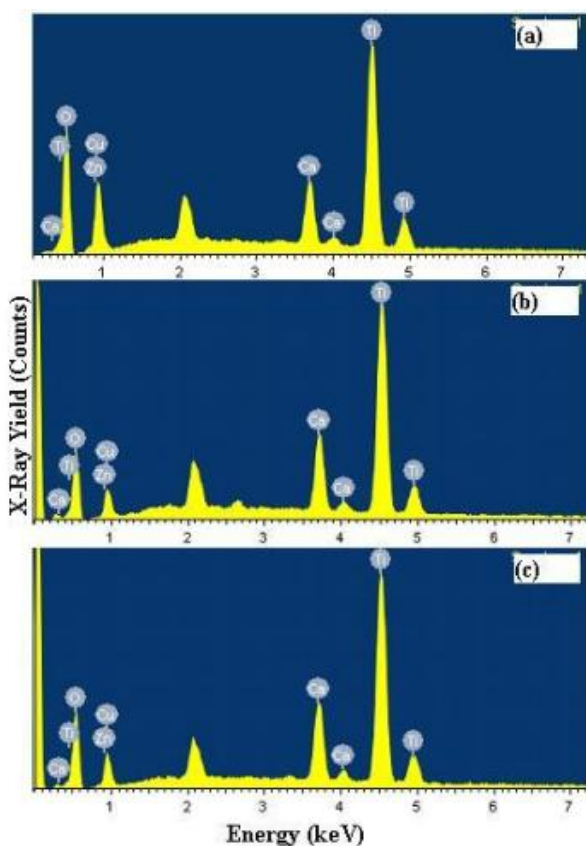


Figure 6. EDX spectrum of CCZTO ceramics sintered at 950 °C for (a) 6h , (b) 8h and (c) 12h

The temperature dependence of dielectric constant (ϵ_r) and loss tangent ($\tan\delta$) of the CCZTO ceramic sintered for 6h at different frequencies 0.1, 1, 10 and 100 kHz are shown in Fig.7. Dielectric constant (ϵ_r) exhibits a step like increase from low value 4216 to a giant value 16560 at temperature above 350K, which is prominent in the low frequency region and diminishes on increasing the frequency. At above room temperature a broad dielectric peak appears between 350K to 425K which also shifts to higher temperature and decreases in amplitude with increasing higher frequencies. It shows a ferroelectric relaxor behavior in the ceramic [25]. It is observed from the Fig. 7 (b) that the corresponding peaks are also present in the temperature-dependent plot $\tan\delta$. The above characteristic behaviors of a ferroelectric relaxor is usually characterized by diffuse phase transition and strong relaxational dispersion in dielectric constant and loss tangent ($\tan\delta$).

Figs.8 & 9 show the variation of dielectric constant and loss tangent ($\tan\delta$) with temperature at 0.1, 1, 10 and 100 kHz for CCZTO ceramics sintered at 950 °C for 8h and 12h, respectively. It is clearly shown from the figure that ferroelectric behavior is not present. It is also observed that the dielectric constant and dielectric loss of CCZTO 8h and 12h are temperature independent at higher frequency whereas temperature dependent in the low frequency region. It is also noted from the figures that the values of ϵ_r for CCZTO ceramic are 1083, 4751 and 4957 at 1kHz for 6h, 8h and 12h, respectively.

It is also inferred that ϵ_r increases with increasing sintering time. This is due to the fact that the longer sintering time produces more oxygen vacancies in the CCZTO ceramics and results high dielectric constant. It is observed from the figure that dielectric losses at 1 kHz for CCZTO are 1.07, 0.38 and 0.18 for 6h, 8h and 12h, respectively, at room temperature. A very clear picture of the sintering time dependence of dielectric constant value measured at 10 kHz is shown in Fig. 10. The high dielectric constant for CCZTO ceramics is due to interfacial space charge polarization [26]. This interfacial charge polarization arises due to accumulation of charge carriers at the interface of semiconducting grains and insulating grain boundary.

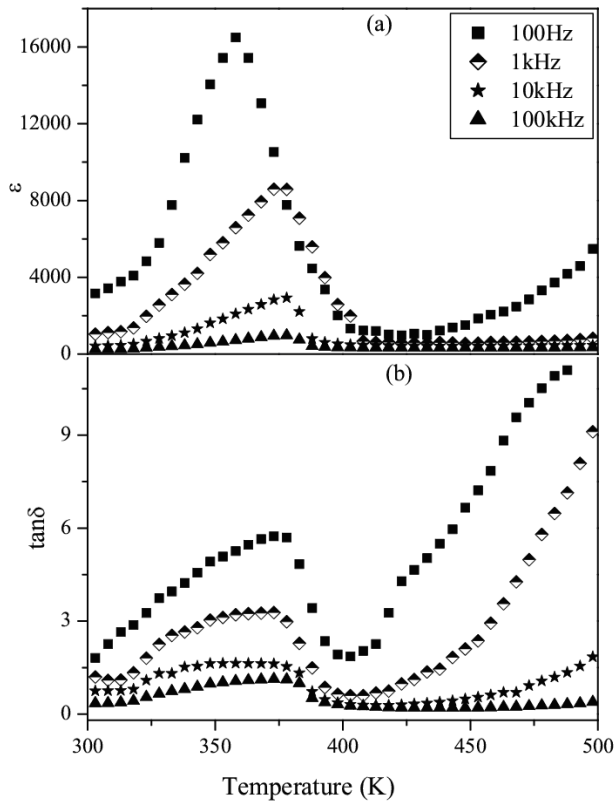


Figure 7. Variation of ϵ_r and $\tan\delta$ vs temperature of CCZTO ceramic sintered at 950 °C for 6h

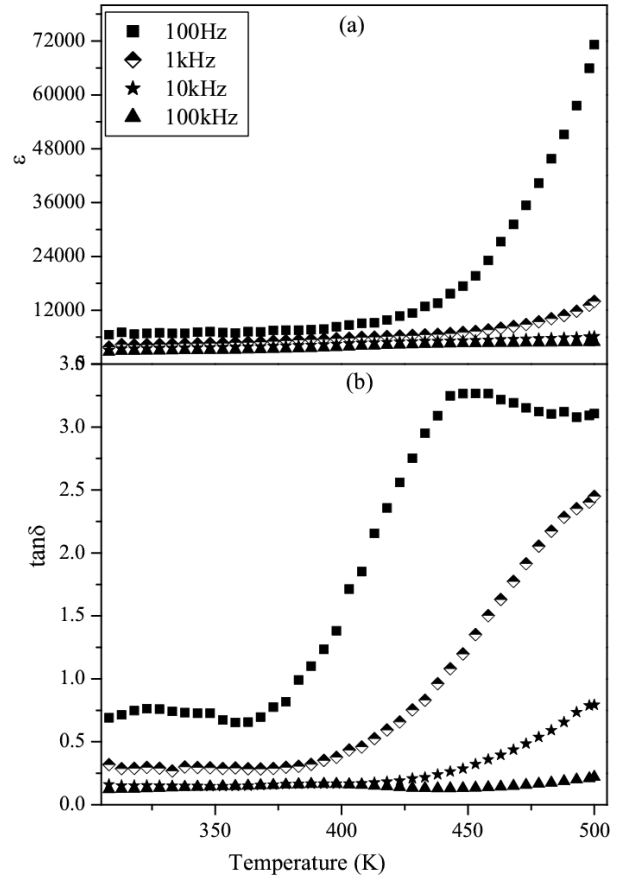


Figure 9. Variation of ϵ_r and $\tan\delta$ vs temperature of CCZTO ceramic sintered at 950 °C for 12h

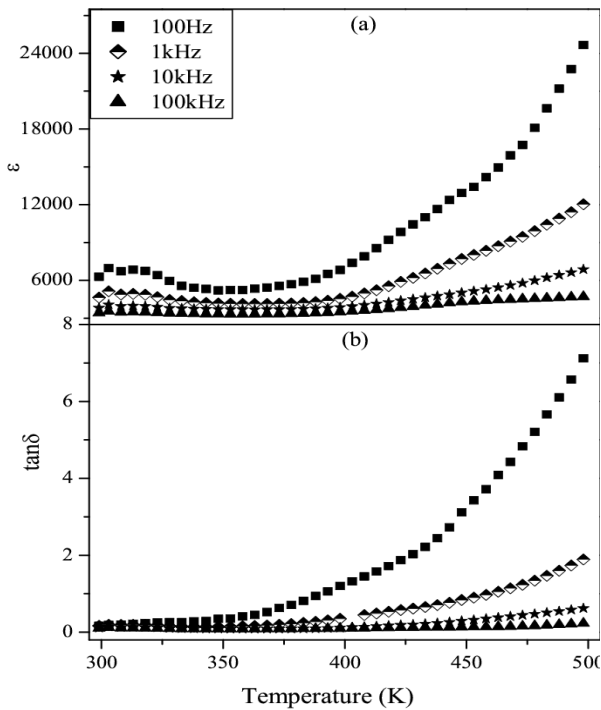


Figure 8. Variation of ϵ_r and $\tan\delta$ vs temperature of CCZTO ceramic sintered at 950 °C for 8h

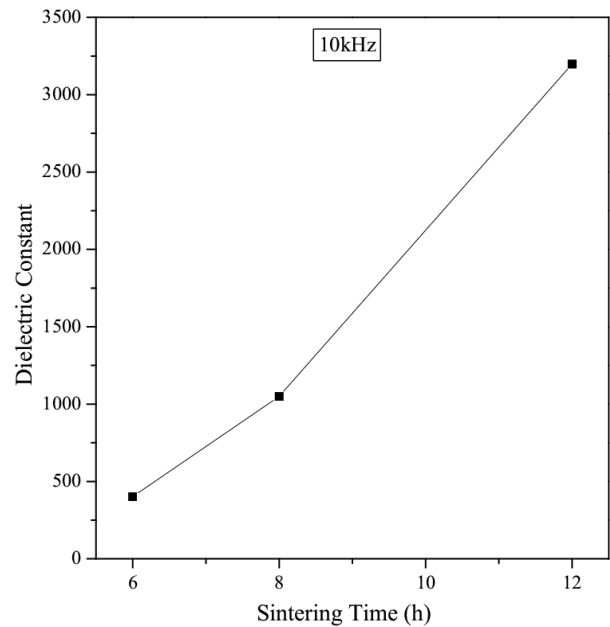


Figure 10. Dielectric constant value as a function of sintering time measured at 10 kHz

4. Conclusion

It is immensely important that an adequate control of sintering time and temperature are needed to obtain the desired microstructure and dielectric properties. Dielectric constant increases with increasing sintering time and dielectric loss decreases. It is suggested that the longer sintering time may lead to more defect structures. The size of the particle increases with increasing sintering time. It is mainly due to formation of large size particles as a result of loss of grain boundaries of small size particles. These changes lead to stability to the large size particles due to loss in grain boundary.

5. Acknowledgements

Authors express their gratitude to Dr. Madhu, Scientist, Institute of Medical Science, BHU, Varanasi for extending the facility for TEM analysis.

6. References

- [1] X.J. Chou, J.W.Zhai, H.T.Jiang, X.Yao, "Dielectric properties and relaxor behaviour of rare earth (La, Sm, Eu, Dy, Y) substituted barium zirconium titanate ceramics," J. Appl. Phys., Vol.102, pp.084106-084112, 2007
- [2] C.Zhao, X.Y.Huang, H.Guan, C.H.Cao, "Effect of Y_2O_3 and Dy_2O_3 on dielectric properties of $Ba_{0.7}Sr_{0.3}TiO_3$ series capacitor ceramics," J. Rare Earths, Vol. 25, pp.197-200, 2007.
- [3] P.Liu, Y.He, G.Q.Zhu, X.B.Bian, "Influence of Nb doping on the dielectric properties of $CaCu_3Ti_4O_{12}$ ceramics," Acta Physica Sinica, Vol. 56, pp. 5489-5493, 2007.
- [4] C.C.Home, T.Vogt, S.M.Shapiro, S.Wakimoto, A.P.Ramirez, "Optical responses of high-dielectric-constant perovskite related oxide," Science, Vol.293, pp.673-676, 2001.
- [5] S.Y.Chung, S.Y.Choi, T.Yamamoto, Y.Ikuhara, S.J.L. kang, "Change in cation nonstoichiometry at interfaces during crystal growth in polycrystalline $BaTiO_3$," Appl. Phys. Lett., Vol.88, pp.011909-3, 2006.
- [6] S. Kwon, C.C. Huang, E.A. Patterson, E.F. Alberta, W.S. Hackenberger, D.P. Cann, "The effect of Cr_2O_3 , Nb_2O_5 and ZrO_2 doping on the dielectric properties of $CaCu_3Ti_4O_{12}$," Mater. Lett., Vol.62, pp.633-636, 2008.
- [7] W. Kobayashi, I. Terasaki, "Unusual impurity effects on the dielectric properties of $CaCu_{3-x}Mn_xTi_4O_{12}$," Physica B., Vol. 329, pp.771-772, 2003.
- [8] T.T. Fang, L.T. Mei, H.F. Ho, "Effects of Cu stoichiometry on the microstructures, barrier-layer structures, electrical conduction, dielectric responses, and stability of $CaCu_3Ti_4O_{12}$," Acta Mater., Vol. 54, pp.2867- 2875, 2006.
- [9] S.F.Shao, J.L. Zhang, P. Zheng, C.L. Wang, "Effect of Cu-stoichiometry on the dielectric and electric properties in $CaCu_3Ti_4O_{12}$ ceramics," Solid State Commun., Vol.142, pp.281-286, 2007.
- [10] S.D. Hutagalung, L.Y. Ooi, Z.A. Ahmad, "Improvement in dielectric properties of Zn-doped $CaCu_3Ti_4O_{12}$ electroceramics prepared by modified mechanical alloying technique" Journal of Alloys and compounds, Vol.476, pp.477-481, 2009.
- [11] Alok Kumar Rai, K. D. Mandal, D. Kumar and Om Parkash, "Dielectric properties of $CaCu_3Ti_{4-x}Co_xO_{12}$ ($x = 0.10, 0.20, 0.30$) synthesized by Semi-wet Route" Materials Chemistry and Physics, Vol. 122, pp.217-220, 2010.
- [12] M. Li, A. Feteira, D. C. Sinclair and A. R. West, "Influence of Mn doping on the semiconducting properties of $CaCu_3Ti_4O_{12}$ ceramics" Appl. Phys.Lett., Vol.88, pp.232903-912, 2006.
- [13] D. Xu, C. Zhang, X.N. Cheng, Y. Fan, T.Yang and H.M. Yuan, "Dielectric properties of Zn Doped CCTO Ceramics by Sol-Gel Method" Advanced Materials Research, Vol. 197, pp.302-305, 201.
- [14] M. Li, X. L. Chen, D. F. Zhang, W. Y. Wang and W. J. Wang, "Humidity sensitive properties of pure and Mg-doped $CaCu_3Ti_4O_{12}$ " Sensors and Actuators B: Chemical, Vol.147, pp.447-452, 2010.
- [15] M. Li, Gemei Cai, D. F. Zhang, W. Y. Wang, W. J. Wang, and X. L. Chen, "Enhanced dielectric responses in Mg-doped $CaCu_3Ti_4O_{12}$ " Vol. 104, pp.074107-4, 2008.
- [16] R.Aoyagi, M. Iwata, M.Maeda, "Effect of Sintering Temperature on the Dielectric Properties of $CaCu_3Ti_4O_{12}$ Ceramics," Ferroelectrics, Vol.356, pp.90-94, 2007.
- [17] B. Shri Prakash, K.B.R. Varma, "Effect of sintering conditions on the dielectric properties of $CaCu_3Ti_4O_{12}$ and $La_{2/3}Cu_3Ti_4O_{12}$ ceramics, A comparative study, Physica B, Vol. 382, pp.312-319, 2006.
- [18] P.Jha, P.Arora, A.K.Ganguly, "Polymeric citrate precursor route to the synthesis of the high dielectric constant oxide $CaCu_3Ti_4O_{12}$," J.Mater. Lett., Vol.57, pp.2443-2446, 2003.
- [19] J.Liu, R.W. Smith, W.N. Mei, "Synthesis of the Giant Dielectric Constant Material $CaCu_3Ti_4O_{12}$ by Wet-Chemistry Methods," Chem. Mater., Vol.19, pp.6020-6024, 2007.
- [20] C.Masingbon, P.Thongbai, S.Maensiri, T.Yamwong, S.Seraphin, "Synthesis and giant dielectric behavior of $CaCu_3Ti_4O_{12}$ ceramics prepared by polymerized complex method," Mater. Chem. Phys., Vol. 109, pp.262-270, 2008.
- [21] D. Kaur, S. B. Narang, "Influence of increased sintering time on structure and dielectric behaviour of barium lanthanide titanates", Ceramics-Silikaty, Vol. 54, pp.108-115, 2010.

- [22] B.D. Cullity, S.R. Stock, "Elements of X-ray Diffraction, Prentice Hall, New Jersey, Chapter 1, pp. 7-10, 2001.
- [23] D.W. Kim, T.G. Kim and K.S. Hong 'Low firing of CuO doped anatase' Mater. Res. Bull. Vol. 34, pp.771-781, 1999.
- [24] C.L. Huang, and Y.C. Chen, 'Low temperature sintering and microwave dielectric properties of SmAlO₃ ceramics' Mater. Res. Bull. Vol. 37 pp.563-574, 2002.
- [25] M.Veith, S.Ren, M. Wittmar, H. Bolz, "Giant dielectric constant response of the composites in ternary system CuO-TiO₂-CaO," J.Solid State Chem., Vol.182 pp.2930-2936, 2009.
- [26] H. Birey, "Dielectric properties of aluminum oxide films," J. Appl. Phys., Vol. 49, pp.2898-2904, 1978.